Prediction of Lead-Acid Battery Performance Parameter: An Neural Network Approach

E. Jensimiriam*, P. Seenichamy, S. Ambalavanan
Lead-acid battery Group, Central Electrochemical Research Institute, India.
*Corresponding author, e-mail: jensisandhya@gmail.com

Abstract

In real-time applications life of lead-acid battery are affected by many factors such as state of charge, rate of charging /discharging, temperature and aging. If these factors of battery are frequently encountered thought-out the lifecycle, battery performance degradation is identified. Hence, in this communication a valve regulated lead-acid batteries (VRLA) electrical behavior are modeled using MATLAB/SIMULINK and the performance parameters related to the battery such as internal resistance (R), state of charge (SOC), and capacity under various operating conditions are predicted using artificial neural network (ANN). The relevant simulation results are compared with experimental results. A validation result shows that this model can accurately simulate the dynamic behavior of the lead-acid battery for any different experimental data sets. This paper describes initial feasibility studies as well as current models and makes comparisons between predicted and actual performance.

Keywords*: Lead acid battery, neural network simulation, secondary battery model, parameter prediction.*

1. Introduction

The recent rapid expansion in the use of portable electronics, computers, personal data assistants, cellular phones, power tools, and even electric and hybrid vehicles creates a strong demand on fast deployment of battery technologies at an unprecedented rate. In today's highly computerized society, communications lines must be sustained even in the event of an outage of the commercial power supply [1]. Accordingly, as a means of supplying power to communications facilities and equipment during such a power outage, lead-acid batteries are generally used. Unlike a flooded-type lead-acid battery, the valve-regulated lead-acid battery does not require maintenance work such as re-filling with water. Moreover, the way in which it can be set up is unrestrained, and its lifetime has been extended through various developments. Owing to these advantageous features, introduction of VRLA batteries is being speeded up [2-3].

In this paper simulation of dynamic model of 12V/65Ah VRLA battery is analyzed. Battery comprises a complex set of interacting physical and chemical processes. It is difficult to model accurately. Researchers have developed numerous computationally feasible mathematical models that capture battery behavior in sufficient detail. Physical models provide a detailed description of the physical processes occurring in the battery. Empirical models consist of ad hoc equations describing battery behavior with parameters fitted to match experimental data. Abstract models represent a battery as electrical circuits, discrete-time equivalents, stochastic process models, and so on. Mixed models offer a simplified view of the physical processes with empirically fitted parameters. Besides, unpredictability and uncertainty associated with operator's behaviors also add difficulty to estimate battery parameters accurately. Therefore, a variety of algorithms has been proposed to estimate battery parameters. The method of charge counting or current integration is presently the most commonly used one. However, the battery parameters vary with type and experimental conditions and their variation is not uniform for all battery systems [4-5].

Basically there are three types of battery models reported in the literature, specifically: experimental, electrochemical and electric circuit-based. Experimental and electrochemical models are not well suited to represent cell dynamics for the purpose of state-of charge estimations of battery packs. However, electric circuit-based battery model represents an

electrical characteristic of the battery. There are many types of electric circuit-based battery models reported in literatures. As an alternative approach, we have developed non-phenomenological models for secondary battery systems based on artificial neural networks. For performance study, common modeling approach is to develop an electrical circuit that is designed to be functionally equivalent to the battery. The accuracy of these models depends upon the number of characterization tests performed to identify the values of the circuit elements [6-7].

In this paper, we have developed a technique which uses short term information to predict long term information with the measured data. For this, artificial neural network with specifically feed-forward back propagation algorithm is developed. ANN overcomes the limitations of the conventional approaches by extracting the desired information directly from the experimental data. The fundamental processing elements are neurons. A schematic structure of the ANN is shown in Figure 1. Network is a parallel distributed information processing technique. In this Configuration, networks are arranged in layers, with the first layer taking in inputs and the last layer producing outputs. The middle layers have no connection with the external world, and hence it is called hidden layers. Each layer is connected with Neurons in between them. The sizes of middle (hidden) layers are determined by trial and error methods. A typical ANN operation starts with the training stage, which modifies the connection weights in some orderly fashion using a suitable learning method [8-10]. To train this network, back propagation algorithm based on experimental result is used.
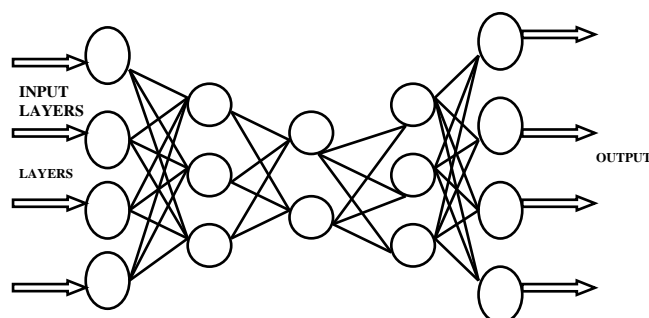

Figure 1. Schematic diagram of general Artificial Neural Network structure

Accurate results can be obtained with the choice of smallest number of neuron for a given problem. The single or multiple inputs are applied from the sensor or previously recorded data to the input layer with each of the inputs are multiplied by a weight and the product summed. The summation of the weighted input is passed through sigmoid function which is activation function. The algorithm updates the network weights in such a way that the sum - squared error in network's result is minimized. The architecture, activation function and learning algorithm are the important characteristics of the ANN model. Back propagation is the generalization of the Widrow-Hoff learning rule to multiple-layer networks and nonlinear differentiable transfer functions. Input vectors and the corresponding target vectors are used to train a network until it can approximate a function, associate input vectors with specific output vectors, or classify input vectors in an appropriate way as defined by user. Networks with biases, a sigmoid layer, and a linear output layer are capable of approximating any function with a finite number of discontinuities [11-13].

2. Research Method

A simple, fast, and effective circuit model structure for lead - acid batteries as shown in Figure 2 has been described. The structure did not model the internal chemistry of the lead - acid battery; instead the equivalent circuit empirically approximated the behavior at the battery terminals.
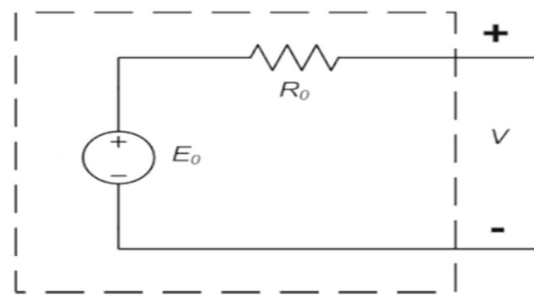
Figure 2. Structure of effective equivalent circuit model of Lead-acid cell

To obtain an electrical model that accurately reproduces the battery's voltage response over time, a dynamic model is needed. Expanding from the very basic static circuit model developed, which adds n sets of parallel R-C components [14-15]. The time constants associated with these RC pairs help shape the battery's dynamic voltage response. The dynamic response test is a relatively new technique that takes a more sophisticated approach to characterizing battery electrical behavior. The purpose of this test is to model the battery's dynamic voltage response to a specific load over a predefined period. System identification techniques are used to estimate parameter values for a selected electrical model that enable accurate reproduction of the measured voltage response of the battery. Changes in a battery's dynamic electrical behavior, manifested as changes in estimated parameter values, is indicative of chemical and morphological transformations occurring within the battery. According to Kirchhoff's voltage law (KVL) and Kirchhoff's current laws (KCL) define the behavior of the model [16-18]. The Figure 3 gives circuit for KCL and KVL.
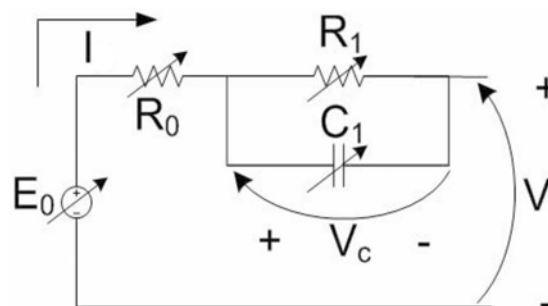

Figure 3. Equivalent circuit according to KCL and KVL.

The current in this model is positive when leaving the positive electrode (discharge), and negative when entering the positive electrode (charge).The resistance term $R_0$is often referred to as the 'high-frequency' resistance, as it is the only impedance to current/ion flow that will be encountered under high frequency loads. This resistance is always present, and can be attributed to ohmic losses in the electrode grid. The steady-state resistance R that is encountered under DC conditions after the initial transient subsides is the sum of $R_0$and R_1. Therefore, R_1can be thought of as an additional equilibrium resistance associated with: charge-transfer processes, ionic diffusion, electrolyte concentration gradients, and active material. Process of the parameter estimation for calculation of R_0, R_1, and R2 is done in MATLAB .these parameters are estimated using a nonlinear least squares minimization. Simulink was used to simulate this battery model. R_0 value formulated as:

R_0 = R_{00} [1 + A_0 (1 – SOC)]
R_{00} - value of R_0 at SOC=1 in Ohms.

Where;

A$_0$ - Constant.
SOC   - State of charge

R$_1$ Value formulated as:

R$_1$ = - R$_0$ ln (DOD)
Where:

R$_{10}$ -   Constant in Ohms.
DOD - Depth of discharge.

The time constant modeled a voltage delay when battery current is changed

C$_1$ = τ$_1$ / R$_1$

τ$_1$ = Time constant

Therefore, battery internal resistance is:

R = R$_0$ +R$_1$

An increase in the ohmic resistance of the battery is also observed with battery ageing. Experimentally, the resistance is calculated by dividing the time average value of the active power by the time average of the square of the battery current. For parameterization method of lead acid battery, it required standard experimental test data. For discharge, full batteries were discharged at constant currents and temperatures. For charge, batteries were charged at constant current, until the terminal voltage approached the gassing voltage for the battery. Then, the charges were continued at constant voltage, until the batteries reached a full charge. Several typical currents, voltage and ambient temperatures were used for the testing procedure.
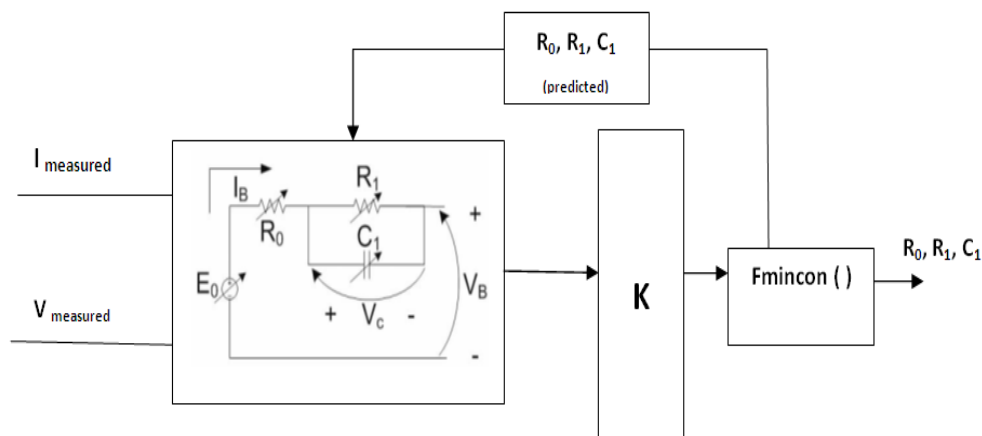

Figure 4. Model for Parameter Estimation

Steps involved in parameter Estimation:
- Measure battery current and temperature over time,
- Calculate voltage response using estimated parameters,
- Compare calculated voltage response to measured voltage mainly focus on the linear part of the characteristics.
- Adjust estimated parameters with help of difference in target output.
- Deduct information about battery state from adjusted parameters.
    A quantification of performance degradation in terms of capacity reduction caused by aging mechanisms may also be possible with this diagnostic technique. The dynamic response

test consists of: data collection, parameter estimation. An open-circuit voltage measurement collected at this point serves as an estimate of battery SOC and provides a value for E_0. Next, parameters R_0, R_1 and C_1 are estimated using a nonlinear least squares minimization. Simulink was used to simulate this battery model. A MATLAB script was used to calculate the least squares error between measured and modeled voltages. The goal of this dynamic response test is to determine a relationship between one or more of the estimated parameters and the battery capacity. If such a relationship can be found, the dynamic response test could be conducted on a battery of unknown state, and the parameter values estimated from the test's voltage and current measurements could be used to determine the capacity of the battery. Each equivalent circuit element was based on non linear equations. The nonlinear equations included parameters and the parameters of the equations were dependent on empirically determined constants. This iterative process is performed in designed ANN network and begins by calculating the model voltage output from the measured current input and an initial guess of the parameter values for R_0, R_1 and C_1. This model voltage output is then compared with the measured voltage output at each time instance *by* taking the sum of squares error between the two voltages. An optimization function then attempts to minimize k *by* refining the candidate parameter values in an iterative fashion until a local minimum for k *is* found. The final set of candidate parameter values at the end of this process is taken as the estimate for R_0, R_1 and C_1.

2.1. Measurements of the Battery Characteristics: Experimental Set Up

The battery modeling using artificial neural network was based on experimentally measured characteristics of the battery. The capacity of the valve-regulated lead-acid battery used in this experiment is 12V/65Ah.The internal resistance of VRLA battery is monitored during cycling at constant rate of discharge C_{10}, C_5 and C_3 in order to determine the resistance variation and monitoring the SOC (state of charge) with the parameter. It is noted that at lower discharge rate, R value is increased only a low SOC and at a high discharge rate R value increases linearly. Our experiments carried out at room temperature without any specific temperature control. The charge and discharge series were run using an LCN programmable tester, manufactured by Bitrode Corporation which is designed to test as per the standards such as BCI, SAE, DIN, JIS, IEC, and BS. The following experiments are carried out for our study. Consider fully charged battery 12V/65Ah; Discharge it by changing the current in step wise manner shown below until the battery reach 10.5V.

Case I: SOC = 100%
1. Discharge the battery at I (current) = 0.2C (13)A ;
2. Then charge the battery at I=0.1C A to attain the 100%.
3. Discharge the battery at I = 0.4C (26) A;
4. Then charge the battery at I=0.1C A to attain the 100%.
5. Discharge the battery at I = 0.6C (39) A;
6. Stop

Case II: SOC = 75%
1. Discharge the battery at I = 0.2C A ;
2. Then charge the battery at I=0.1C A to attain the 75%.
3. Discharge the battery at I = 0.4C A
4. Then charge the battery at I=0.1C A to attain the 75%.
5. Discharge the battery at I = 0.6C A
6. Stop

Case III: SOC = 50%
1. Discharge the battery at I = 0.2C A ;
2. Then charge the battery at I=0.1C A to attain the 50%.
3. Discharge the battery at I = 0.4C A
4. Then charge the battery at I=0.1C A to attain the 50%.
5. Discharge the battery at I = 0.6C A
6. Stop

Measures battery voltage, internal resistance, and Ah output for every step of discharge. The unit voltage, time, current, temperature, watt-hour and ampere- hour and number of cycles achieved with discharge – charge cycle shall be recorded.

2.2. Calculation Of Discharge Resistance Using Experimental Data Set

R depends on both SOC and the direction of current flow (I). Hence the OCV and SOC (0-1) is noted and voltage mapping is drawn,

The energy removed from the battery during time interval 't' is designed as

$$Q = \Delta t \, (I^2 * R + V * I);$$

Hence, new battery SOC reduces to:

$$SOC = 1 - (I * \Delta t / Q);$$
$$Voc = a + b \, SOC - c \, ((I^2 * R + V * I);$$

Where $c = b \, (\Delta t)/Q$

Hence, internal resistance is calculated as:

$$R = (-V / I) + (a + b * SOC) / I \, (1 - c * I)$$

Battery mapping to find V_{OC}

In order to estimate any of the aforementioned battery performance metrics, extensive electrical characterization parameter derived from empirical data under different conditions battery mapping is used. One of the most fundamental and important of these 'maps' or tables is the relationship between battery rested open-circuit voltage and amp hours discharged. Using the charging protocol specified by the battery manufacturer, the battery should first be fully charged. This ensures that the maximum amount of active material is available for reaction. After a 24 hour rest period, the first open-circuit voltage should be recorded. At this point, the battery should be discharged at the C_{20} rate for a period that would correspond to a 10% change in SOC. Battery Mapping done at C_{20} discharge rate with 10% change in SOC is shown in the Figure 5.
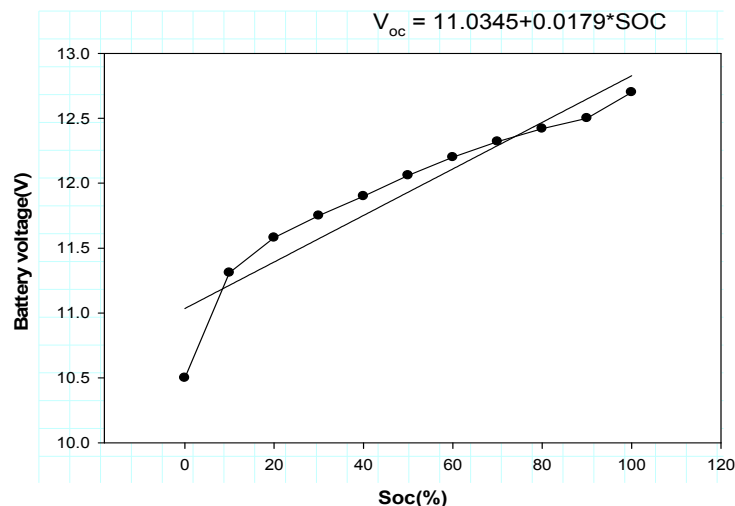

Figure 5. Battery Mapping done at C_{20} discharge rate with 10% change in SOC.

The figure below shows the relation between the internal resistance with respect to voltage and state of charge of a particular battery at specifies operating conditions.
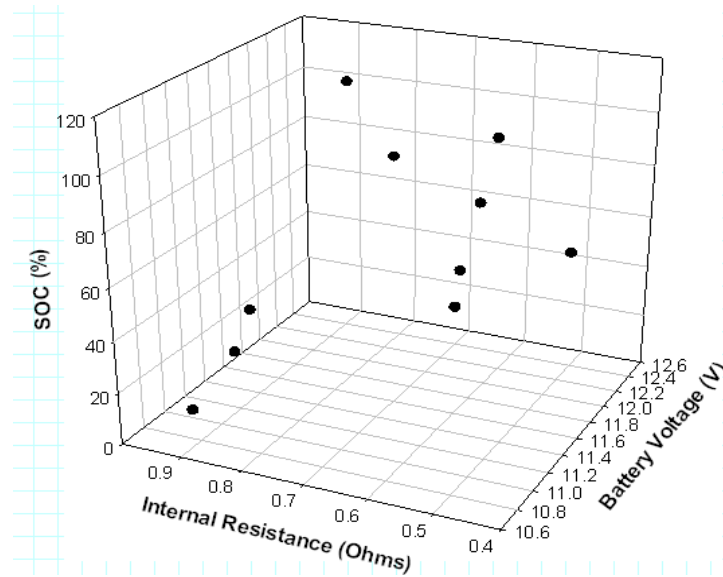
Figure 6 shows the relation between the internal resistance with respect to battery voltage and state of charge (0 to 100 %)

3.3 Simulation Results

The error is calculated as the difference between the experimentally target output and the designed network output. The goal is to minimize the average of the sum of these errors. The values of mean square error (MSE) that indicate of the models performance to represent the battery behavior during the processes are given in Table 1 calculated with the equation

$$.MSE = \left[\frac{1}{N} \sum_{i=1}^{N} \left[\frac{C_i - M_i}{M_i} \right]^2 \right]^{1/2} \times 100$$

Where C_i and M_i are the computed values and measured, respectively,

Table 1. Sum square error value and correlated value of Measured and predicted data at different discharge rate.

C_3 (Discharge Rate)		C_5 (Discharge Rate)		C_{10} (Discharge Rate)	
Error	R^2	Error	R^2	Error	R^2
0.396	0.9056	0.026	0.9323	1.96	0.9012

Comparison between battery voltage and internal resistance for measured and modeled parameter at different discharge rate is shown in the Figures 7-9.
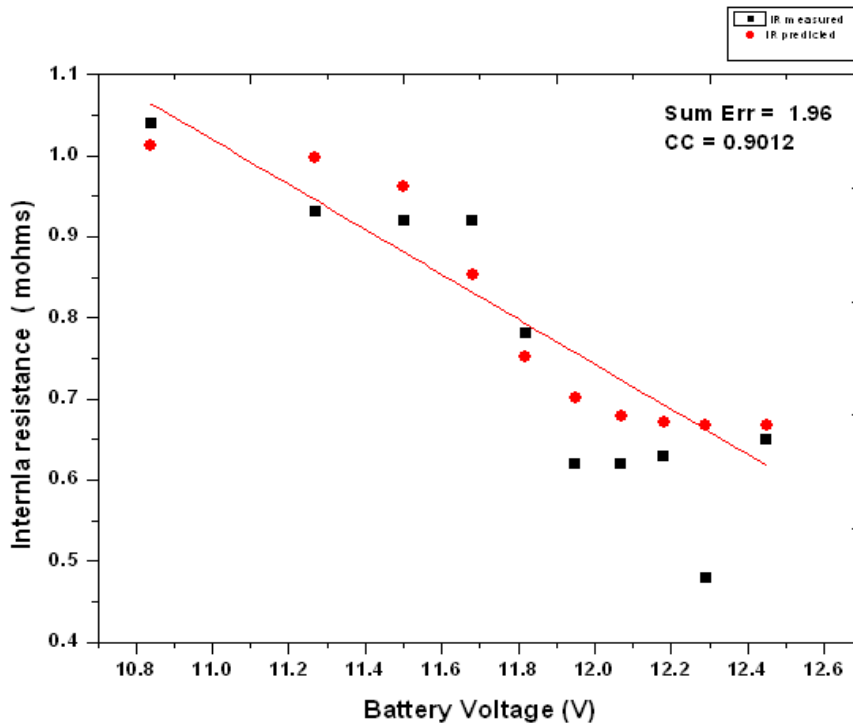
Figure 7. Comparison between battery voltage and internal resistance for measured and modeled parameter at C_{10} Discharge Rate
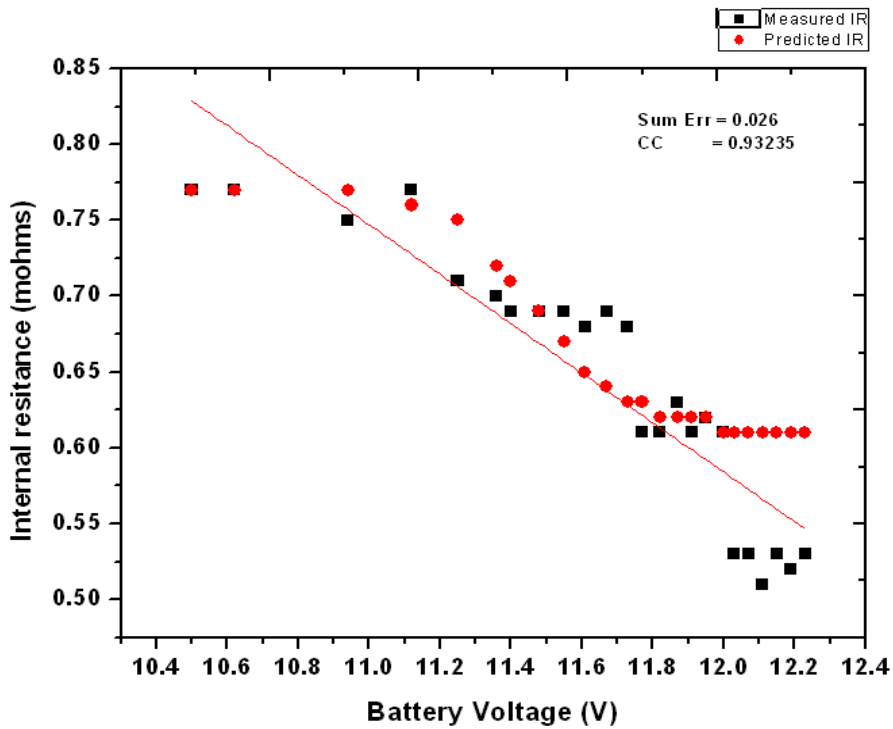

Figure 8. Comparison between battery voltage and internal resistance for measured and modeled parameter at C_5 Discharge Rate
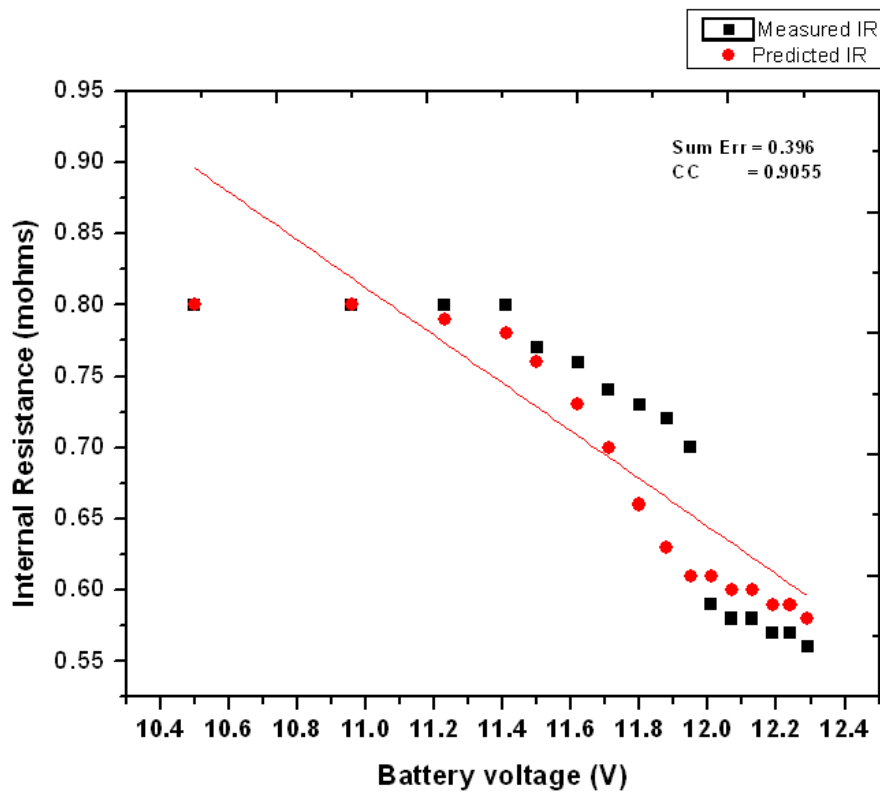
Figure 9. Comparison between battery voltage and internal resistance for measured and modeled parameter at C_3 Discharge Rate.

However, cell performance also affected by deterioration of the active chemicals as the battery ages. Although there are many failure modes of VRLA batteries, including premature capacity loss, grid corrosion, softening, sulfation, drying out, additive decomposition and poor separator plate contact, etc., they vary with different designs, manufacturing and operating conditions. The lead-acid battery ageing causes an increase of its resistance and thus a decrease of its available capacity. Therefore, the battery resistances are simulated and the effects of State of Charge (SOC) on internal battery resistance were examined and showed that as the SOC decreases, the battery resistance increases, which can be justly related to physical interactions inside the battery.

4. Conclusion

In this communication, dynamic behavior of lead-acid battery models using artificial intelligence is investigated and presented. Hence, in this study valve regulated lead-acid batteries electrical behavior are modeled using MATLAB/SIMULINK and the performance parameters related to the battery such as internal resistance, state of charge, and capacity under various operating conditions are predicted using artificial neural network. The relevant simulation results are compared with experimental results. Validation results show that this model can accurately simulate the dynamic behavior of the lead-acid battery for any different experimental data sets. This model works fast and the accuracy of this method verified by using the experiment. The presented method can be extended for other different equivalent circuit models, and also can be modified to simulate the battery characteristics by entering other battery parameters

References

1. Bernardi D. M., H. Gu and A.Y. Schoene. Two-dimensional mathematical model of a lead-acid cell. *J. Electrochem. Soc.*, 1998; 140(8): 2250-2258.
2. Culpin B. D. and A. J. Rand .Failure modes of lead/acid batteries. *J. Power Sources.*1991; 36(2): 415-438.
3. Krein P.T. and R.S. Balog. *Life extension through charge equalization of lead-acid batteries.* In Proc. IEEE INTELEC'02. 2002: 516-523.
4. Jackey, Robyn A. *A Simple, Effective Lead-Acid Battery Modeling Process for Electrical System component Selection.* SAE Paper 2007-01-0778, SAE International, Warrendale, PA, 2007.
5. P. Rüetschi .Review on the lead–acid battery science and technology. *J. Power Sources.* 1977-1978; 2: 3–24.
6. K. Takahashi, M. Tsubota, K. Yonezu, K. Ando. Physical changes in positive active mass during deep discharge–charge cycles of lead–acid Cells. *J. Electrochem Soc.* 1983; 130: 2144–2149.
7. J. Alzieu, N. Koechlin, J. Robert. Internal stress variations in lead–acid batteries during cycling. *J. Electrochem. Soc.* 1987; 134: 1881–1884.
8. Barr A, Feigenbaum EA. The handbook of artificial intelligence. Los Altos, CA: Morgan Kaufmann; 1981(1).
9. Kalogirou SA. Artificial intelligence for the modeling and control of combustion processes: a review. *Prog Energy Combust Sci.* 2003; 29: 515–66.
10. Medsker LR. Microcomputer applications of hybrid intelligent systems. *J Network Computer Applications.*1996; 19: 213–34.
11. Rich E, Knight K. Artificial intelligence. McGraw-Hill: New York .1996.
12. Konar A. Artificial intelligence and soft computing behavioral and cognitive modeling of the human brain. 1999. Boca Raton, FL: CRC Press.
13. Deyi L, Yi D. Artificial intelligence with uncertainty. First ed. London: Chapman & Hall/CRC; 2007.
14. Wu B., Dougal R., White R.E. Resistive companion battery modeling for electric circuit simulations. *J. Power Sources.* 2001; 93: 186-200.
15. Piller S., Perrin M., Jossen A. Methods for state-of charge determination and their applications. *J. Power Sources.* 2001; 96: 113-120.